

Wearable Self-Charging Power Textile Based on Flexible Yarn Supercapacitors and Fabric Nanogenerators

Xiong Pu, Linxuan Li, Mengmeng Liu, Chunyan Jiang, Chunhua Du, Zhenfu Zhao, Weiguo Hu,* and Zhong Lin Wang*

Personal electronics are advancing toward an era when the pursuit of multifunctionality and wearability will become the most important trend. This advancement requires not only miniaturization of the size of various electronic components, but also more importantly incorporating them into cloth fabrics and accessories (watch, eyeglass, bracelet, etc.), or even implanting them into human body.^[1] The subsequently increasing demand for lightweight, highly flexible, stretchable, and washable power modules is essentially one of the critical challenges for the progress of wearable smart electronics.^[2] Moreover, conventional energy storage devices (batteries and supercapacitors) require frequent and inconvenient charging. Therefore, wearable self-charging power systems that combine energy-harvesting and energy-storing technologies could be potential solutions.

Scheme 1 shows our proposed self-charging power textile that in one individual cloth integrates three functional units: triboelectric nanogenerator (TENG) fabric for energy harvesting, supercapacitor fabric for energy storage, and wearable electronics or sensors (e.g., a button). The intermittent energy generated from the human motion is stored in the textile energy-storing cells for stable power supply to smart electronics in the form of either textile or accessories. The disadvantages of unstable output of energy generators and the short operational time of energy-storing cells can thus be simultaneously overcome.

With regard to energy storing devices, supercapacitors, comparing to current bulky and rigid batteries, show more promising prospects, owing to their high power density, stable cycling life, good safety, and potentials in integration into flexible wears.^[3] Recently, 1D supercapacitor yarns or fibers have been intensively investigated because these 1D building blocks can be readily incorporated into human wearables with arbitrary shapes and high flexibility.^[4] The core challenge is to fabricate lightweight, mechanically strong, and electrically conductive yarns with electrochemically active materials coated on

the surface. A variety of strategies have been developed, mainly including wet-spinning^[5] or dry-spinning^[6] of reduced graphene oxide (rGO) fibers^[7] and carbon nanotube (CNT) fibers,^[8] direct use of metal wires^[9] or carbon fibers,^[10] and dip-coating of carbonaceous materials on fabric yarns.^[11] Yet, each of these approaches has some drawbacks, for example, the high cost of dry-spinning CNT fibers and carbon fibers, the low conductivity of rGO fibers and dip-coated fabric yarns, and the heavyweight of metal wires. Therefore, a fabric yarn with a conformal thin layer of metal coating could be ideal for 1D yarn supercapacitor, since it can have high conductivity while maintaining the lightweight and mechanical flexibility of the fabrics.

Among various energy-harvesting devices, TENG has been proven to be able to harvest mechanical energy of human motions at a high efficiency and large output power density.^[12] Comparing with photovoltaic and thermoelectric energy harvesting, mechanical energy is nearly independent to the weather and working environment. Moreover, it is facile to be designed into textile cloths due to its simple structure and huge materials choices.^[13]

Herein, we report a facile and scalable fabrication of an all-solid-state flexible yarn supercapacitor and its integration with a TENG cloth for a self-charging power textile. A conformal Ni layer and rGO film were successively coated on the surface of common polyester yarns (noted as rGO-Ni-yarn). The resulting symmetric yarn supercapacitor achieved both high capacitance (13.0 mF cm^{-1} , 72.1 mF cm^{-2}) and stable cycling performances (96% for 10 000 cycles). Moreover, no significant degradation of performance was observed for 1000 cycles of 180° bending. For the first time, a textile self-charging power system was demonstrated by charging the yarn supercapacitors with a TENG cloth. Our cost-effective and industrially scalable approaches for yarn supercapacitors and self-charging power textiles pave the way for wearable electronics.

Converting common cloth fabric into energy-storing devices (i.e., supercapacitors) is ideal for wearable electronics, since it is cheap, mechanically strong and flexible, and ready for industrially scale-up fabrication. However, it is insulating, and can be neither the current collector, nor the active material in an electrochemical energy-storing device. In this work, highly conductive 1D fabrics were obtained through electroless deposition of Ni coating directly on common polyester yarns, which were then utilized as current collectors for electrodes in all-solid-state yarn supercapacitors, as schemed in **Figure 1a**. The rGO layer was coated on the electrode as active materials. A symmetric yarn supercapacitor was assembled with two rGO-Ni-yarns in parallel, and poly(vinyl alcohol) (PVA)/ H_3PO_4 gel as solid electrolyte and separator.

Dr. X. Pu, L. Li, M. Liu, C. Jiang, Dr. C. Du,
Z. Zhao, Prof. W. Hu, Prof. Z. L. Wang
Beijing Institute of Nanoenergy and Nanosystems
Chinese Academy of Science
Beijing 100083, China
E-mail: huweiguo@binn.cas.cn; zlwang@gatech.edu
Prof. Z. L. Wang
School of Materials Science and Engineering
Georgia Institute of Technology
Atlanta, GA 30332-0245, USA



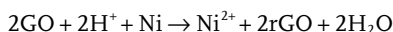
DOI: 10.1002/adma.201504403



Scheme 1. Scheme of a self-charging power textile. It integrates the supercapacitor (SC) yarns as energy-storing fabrics, the triboelectric nanogenerator (TENG) cloth as energy-harvesting fabrics, and wearable electronics (e.g., button sensors).

Through the coating of a Ni thin layer, a polyester yarn with 500 μm diameter was converted to be highly conductive, yielding a length resistance about only 1.48 Ohm cm^{-1} (see Figure S1, Supporting Information), much smaller than that of yarns coated with carbonaceous materials (rGO, SWNT, etc.) with dip-coating or dry-spinning ($\approx 20 \text{ Ohm cm}^{-1}$).^[14] The linear increase in resistance along the length of the Ni-coated yarn (Figure S1, Supporting Information) indicates the uniformity of the Ni-coating. This is especially crucial for scale-up synthesis of long yarn supercapacitors, which require long-distance transfer of electrons. It should also be noted that the weight increase of this coating process is only about $\approx 60\%$, leading to a final density of Ni-yarn of about 2.1 mg cm^{-3} (pristine polyester yarn was measured to be about 1.3 mg cm^{-3}), close to that of carbonaceous materials ($\approx 2.0 \text{ mg cm}^{-3}$) and far smaller than that of metal wires (Ni: 8.9 mg cm^{-3} , Fe: 7.86 mg cm^{-3}). Therefore, high conductivity was obtained without sacrificing the lightweight and mechanical flexibility of pristine fabric yarns.

Figure 1b shows a 1 m long Ni-coated yarn spinning around a cylinder. Figure 1c is an optical photo comparing the pristine polyester yarn, the Ni-coated yarn, and the rGO-Ni-yarn. The white polyester yarn changed into silver with Ni coating, and finally into black with rGO coating. The rGO film was obtained by direct hydrothermal reaction of the Ni-coated yarn in GO aqueous solutions. Spontaneous reduction of GO by many metals (Ni, Zn, Cu, Co) has been demonstrated through the following reaction^[15]



The released Ni^{2+} ion will attract the negatively charged GO from the surrounding solution for further reduction and assembly of rGO on the Ni film, resulting in an rGO hydrogel film on the yarn. After this process, further reduction by ascorbic acid was performed to improve the conductivity of the coated rGO film. Raman spectroscopy of final rGO (Figure S2a, Supporting Information) exhibits an intensity ratio of D (1350 cm^{-1}) to G (1580 cm^{-1}) band of $I_D/I_G > 1$, indicating the reduction of the GO.^[16] X-ray diffraction (XRD) spectra (Figure S2b, Supporting Information) of the final rGO show the absence of the sharp peak of pristine GO at around 10° but a broad peak at about 25° , further confirming the formation of layered rGO sheets. Figure 1d shows the Scanning electron microscopy (SEM) image of a pristine polyester yarn composed of two threads of polyester fibers ($\approx 20 \mu\text{m}$ diameter). With the Ni coating, the pristine morphology is maintained and the total diameter of the yarn is almost unchanged (Figure 1e), indicating the conformal Ni coating. After the rGO coating and further reduction, a thick layer of rGO covers the yarn and the pristine morphology of polyester fibers can hardly be observed (Figure 1f). At higher magnification, the wavy rGO film can be seen on the Ni-coated

polyester fiber (Figure 1g).

Electrochemical performances of the yarn supercapacitor were measured with an all-solid-state symmetric configuration with two rGO-Ni-yarn assembled in parallel and PVA/ H_3PO_4 as a gel-type electrolyte. The cyclic voltammetry (CV) curve keeps a slightly inclined rectangular shape even when increasing the scanning rate up to 1 V s^{-1} (see Figure 2a). The capacitance calculated from the CV curve at 0.01 V s^{-1} is 13.0 mF cm^{-1} (72.1 mF cm^{-2}), which maintains to be 4.4 mF cm^{-1} (24.4 mF cm^{-2}) when increasing the scanning rate two orders higher (i.e., up to 1 V s^{-1}), as shown in Figure S3 (Supporting Information). The yarn supercapacitor was galvanostatically charged/discharged at current densities from 1.0 to 10.0 mA cm^{-2} , showing triangular-shaped profiles (Figure 2b). The specific discharge capacitance at 1.0 mA cm^{-2} was determined to be 8.9 mF cm^{-1} (49.4 mF cm^{-2}), which remains to be 5.0 mF cm^{-1} (27.7 mF cm^{-2}) when increasing the current density 10 times up to 10.0 mA cm^{-2} (see Figure 2c). It is worth noting that only $\approx 1 \text{ s}$ is needed to have a full charge with the current of 10.0 mA cm^{-2} . The excellent capability for high-rate potential scanning and charging/discharging indicates that the Ni coating provides highly conductive paths for electron transfer (see also the small impedance of the yarn supercapacitor in Figure S4 in the Supporting Information). Moreover, stable cycling performance was obtained, achieving a capacitance retention of 96% after charging/discharging at 2.0 mA cm^{-2} for 10 000 cycles (Figure 2d). The charging/discharging profile during the course of the cycling kept the triangular shape and showed no significant degradation (the inset in Figure 2d).



Figure 1. The fabrication of the yarn supercapacitor. a) A scheme of the all-solid-state symmetric yarn supercapacitor composed of two rGO-Ni-yarns in parallel. b) A photograph of a 1 m long Ni-coated polyester yarn. c) A photograph of pristine polyester yarn (white), Ni-coated yarn (silver), and rGO-Ni-yarn (black). Scanning electron microscopy (SEM) images of d) a pristine polyester yarn, e) an Ni-coated yarn, and f, g) an rGO-Ni-yarn. The scale bar is 3 cm for panel (b), 500 μm for panels (d–f), and 50 μm for panel (g).

Table S1 (Supporting Information) compares the specific capacitances obtained in this work with yarn (or fiber) supercapacitors reported in the literature. Since diameters of yarn (or fiber) supercapacitors vary in the literature, areal capacitance is a better parameter for fair comparison. The capacitance of our approach is generally larger than that of yarn supercapacitors made by dry-spinning-aligned CNT on polymer fiber (2.3 and 38 mF cm^{-2} for bare CNT and Polyaniline (PANi)/CNT, respectively,^[17] dip-coating carbonaceous materials (26.4 mF cm^{-2} for pen-ink-coated carbon fiber), or direct using carbon fibers and metal wires (0.6–52.5 mF cm^{-2})^[9c,d,10b,17] It is also comparable with that of rGO fiber (78.7 mF cm^{-2} by Chen et al.^[7b] and 78.3 mF cm^{-2} by Huang et al.^[18] and Poly(3,4-ethylenedioxythiophene) (PEDOT)/CNT fiber (73 mF cm^{-2} by Lee et al.^[8a] synthesized by wet spinning. Kou et al.^[7a] reported a wet-spinning rGO/CNT fiber supercapacitor with an areal capacitance of 177 mF cm^{-2} due to the improved porosity and conductivity by the added CNT. One recently reported yarn supercapacitor with stainless steel wires as substrate showed capacitance of 411 mF cm^{-2} , but large amount of pseudocapacitive species of Polypyrrole (PPy)/ MnO_2 was applied.^[9a] Therefore, the capacitance of the yarn supercapacitor from our approach is among the best performances reported by far. In particular, when an inactive core substrate was utilized, this rGO-Ni-coating showed superiority over many carbonaceous materials and was even comparable with that by using heavy metal wires.

Energy density and power density are two critical parameters of supercapacitors for real applications. As shown by the Ragone plot of Figure 2e, the areal energy density of the yarn supercapacitor was estimated to be 0.54–1.60 $\mu\text{Wh cm}^{-2}$, which is much higher than that of the rGO fiber supercapacitor synthesized by confined hydrothermal reaction (0.17 $\mu\text{Wh cm}^{-2}$),^[19] PANi/CNT fiber supercapacitor by wet-spinning ($\approx 0.56 \mu\text{Wh cm}^{-2}$),^[20] and the dry-spinning PANi/CNT fiber supercapacitor (1.77 $\mu\text{Wh cm}^{-2}$),^[17] and is also comparable with that of the wet-spinning rGO/CNT fiber supercapacitor (3.84 $\mu\text{Wh cm}^{-2}$).^[7a] The areal power density reached 2.42 mW cm^{-2} , which can be about an order of magnitude higher than that of all these four fiber supercapacitors. The high energy density results from the porous structure and large surface area of the rGO film; while the high power density is mainly due to the high conductivity of the Ni coating and the rGO film. Furthermore, compared with reported fiber supercapacitors, our approach requires only three steps of solution-based reactions at low temperature, and is readily viable for scale-up commercialization.

As for wearable energy-storing textiles, the capability to withstand harsh bending or deformation is another important requirement. Therefore, a series of flexibility tests was performed. As shown in Figure S5a (Supporting Information), no degradation of CV at 0.1 V s^{-1} can be observed when the yarn supercapacitor was bent at different angles

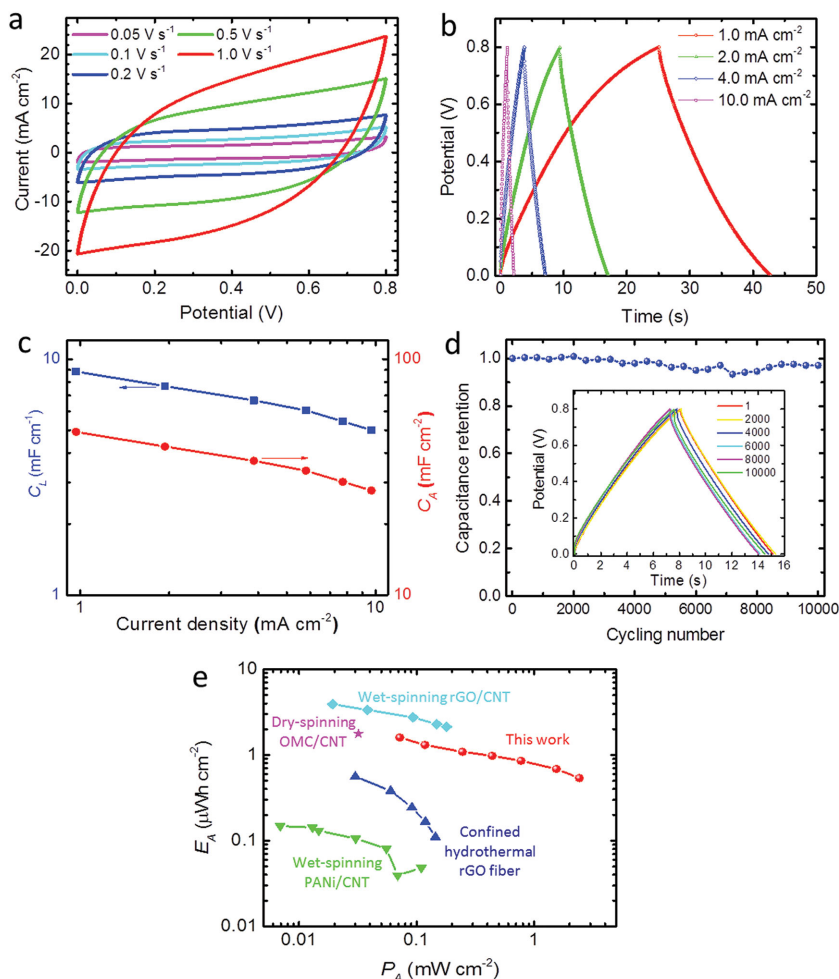


Figure 2. Electrochemical performances of the yarn supercapacitor. a) Cyclic voltammetry (CV) curves of the yarn supercapacitor at different scanning rates. b) Galvanostatic charging/discharging profiles at different current densities. c) The areal and length capacitances summarized from discharging profiles. d) Cycling performances of the yarn supercapacitor. e) Ragone plots comparing areal energy and power densities of the yarn supercapacitor of this work with that of a wet-spinning rGO/CNT fiber supercapacitor,^[7a] a wet-spinning PANi/CNT supercapacitor,^[8d] an rGO fiber supercapacitor by confined hydrothermal synthesis,^[9a] and a dry-spinning order mesoporous carbon (OMC)/CNT fiber supercapacitor.^[9c]

(30°–180°). Slight increases in capacitances (Figure 3a) and corresponding discharging times (inset of Figure 3a) can be found when the yarn supercapacitor was bent, which is probably due to the shortened charge transfer distances through the electrolyte between the two electrodes in a bent state. The yarn supercapacitor was then bended for 180° for 1000 cycles by a linear motor, and the charging/discharging test was performed after every 100 times of bending. The inset in Figure 3b shows a photo of the bended supercapacitor fixed on the linear motor. No significant difference in the charging/discharging profile (Figure S5b, Supporting Information) and the corresponding capacitance (Figure 3b) was observed during the course of bending cycling. These tests confirm the excellent flexibility of the yarn supercapacitor, which is mainly due to the flexible polyester fiber core used, and the intimate and strong binding of the coating materials (Ni and rGO) with the substrate.

The yarn supercapacitor needs to be connected in series and/or parallel so as to increase the voltage and/or capacitance to power real devices. Five yarn supercapacitors connected in series showed a charging/discharging window of 4 V, fivefold of that of a single yarn (0.8 V) but with similar charging/discharging time, as shown in Figure 3c. Overall capacitances of series-connected yarns decrease linearly with the reciprocal of the number of yarns (Figure S6a, Supporting Information). When five yarn supercapacitors connected in parallel, the scanning current increases by a factor of 5 (Figure 3d). The overall capacitance calculated from the CV curve increase linearly with the number of parallel connected yarn supercapacitors (Figure S6b, Supporting Information).

To demonstrate the capability in incorporating our yarn supercapacitors into wearable fabrics, five yarn supercapacitors were connected in series and were woven into a piece of fabric together with common cotton yarns, as shown in Figure 3e. After being charged, this soft energy-storing fabric can light a red light-emitting diode (LED) (Figure 3f). Considering the demonstrated flexibility and weavability of the yarn supercapacitor, it is possible to realize more complicated patterns in a comfortable and fashionable energy-storing fabric.

In order to integrate the yarn supercapacitor into a self-charging power textile, a fabric TENG was designed to harvest energy of human motions. The TENG fabric was woven by using Ni-coated polyester straps and parylene-Ni-coated polyester straps as longitudes and altitudes, respectively. All the parylene-Ni-coated and Ni-coated polyester straps were connected as electrodes A and B, respectively. Figure 4a shows the scheme of the TENG cloth in a contact-separation mode

motion with a common cotton cloth. Figure 4b is a photo of the TENG cloth with the size of 10 × 10 cm². The energy-generating mechanism of the TENG cloth is schematically illustrated in Figure 4c. As the triboelectric negativity of the parylene, cotton cloth, and Ni is different, contact electrification will occur when bring the TENG cloth in contact with the cotton cloth. When they are separated, electric induction effect of electrified charges in the parylene film results in the flowing of electrons between the Ni coatings in the two electrodes of the TENG cloth, yielding a current through the external circuit. Repeated cycling of the contact and separation motions leads to an alternating output, as shown in Figure 4d. The open-circuit voltage has a peak-to-peak value of about 40 V with contact-separation mode motion at 5 Hz; the short-circuit current has a peak value of about 5 μA at 5 Hz. By increasing the motion frequency, the amplitude of the output voltage keeps almost unchanged, while the amplitude of the current increases. The current amplitude

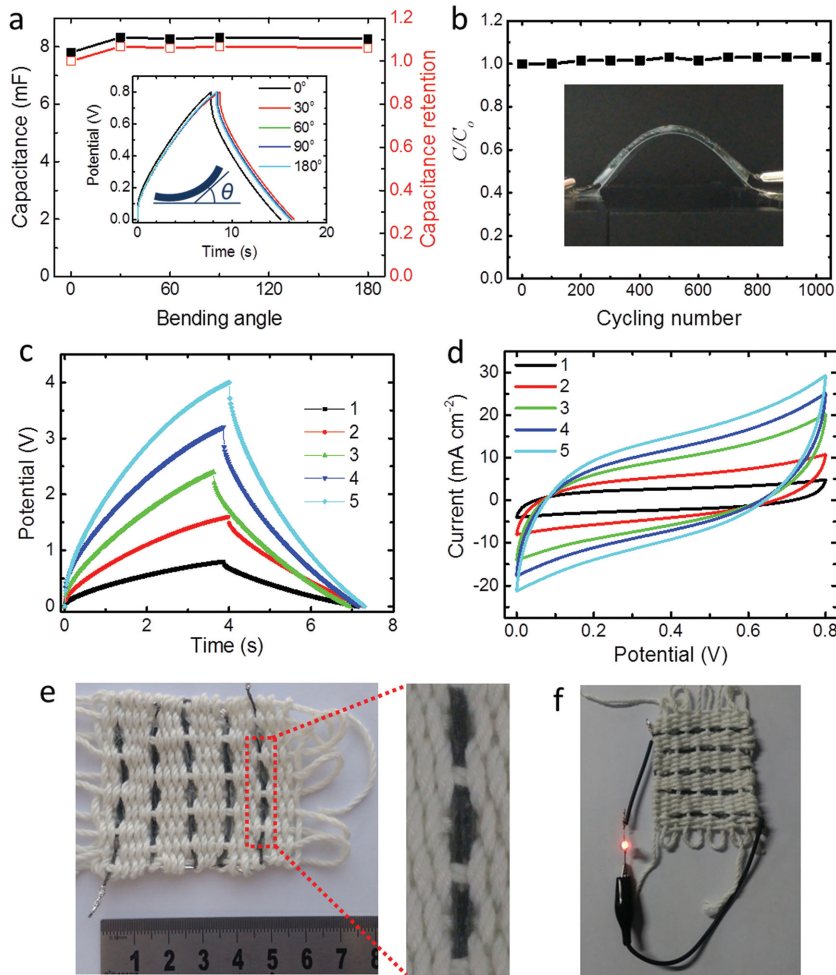


Figure 3. Flexibility and weavability tests of the yarn supercapacitor. a) Discharging capacitances of the yarn supercapacitor at different bending angles. The inset in panel (a) is the corresponding charging/discharging profiles at 2.0 mA cm^{-2} . b) Normalized capacitances of the yarn supercapacitor bended at 180° for 1000 cycles. The inset in panel (b) is a photograph of a bended yarn supercapacitor fixed on a linear motor. c) Charging/discharging profiles of one to five yarn supercapacitors connected in series. d) CV curves of one to five yarn supercapacitors connected in parallel. e) Photograph of a fabric woven with five yarn supercapacitors in series and common cotton yarns, and f) a red LED lit by this energy storing fabric.

is about 10 and $17 \mu\text{A}$ for 10 and 20 Hz, respectively. With a bridge rectifier, the negative portion of the current can be reversed into positive (Figure S7, Supporting Information). The TENG cloth can be worn on many positions of the human body as long as there is a relative motion, for example underneath the arm, on the leg and on the foot. When it was worn on the foot, the rectified current reached an average peak about $\approx 40 \mu\text{A}$ (Figure S8, Supporting Information).

Considering the weavability of both our yarn supercapacitors and TENG cloths, they can be integrated into one individual fabric. Figure 5a demonstrates the viability of the self-charging power textile by weaving a supercapacitor fabric (with three yarn supercapacitors in series-connection) aside a TENG fabric. More complicated design is possible since both fabrics are started from 1D yarn building blocks, so as not to sacrifice the comfort and fashion of a cloth. The equivalent circuit of the self-charging power textile is shown in Figure 5b. A bridge

rectifier was used to rectify the current for the charging of yarn supercapacitors. Though the rectifier is not flexible, it is possible to design it into either a logo or a button of a cloth, considering its small size ($\approx 0.5 \times 0.5 \text{ cm}^2$). We charged the yarn supercapacitor with the TENG cloth in contact-separation motion with a common cloth. The three-series yarn supercapacitor can be charged by the TENG cloth to 2.1 V in 2009 s with a vibration motor at about 5 Hz (Figure 5c). This TENG cloth-charged supercapacitor later can be galvanostatically discharged at $1 \mu\text{A}$ for 811 s, further confirming the validity of our self-charging power textile. When increasing the frequency to 10 Hz, the charging time can be shortened to 913 s, and the following discharge at $1 \mu\text{A}$ can still last for 808 s. It should be noted that further improvement in the charging efficiencies can be achieved by obtaining impedance matching between the TENG and yarn supercapacitors, since the internal impedance of the TENG is generally several orders higher than that of energy-storing devices.^[21] Our recent works have shown that up to 72.4% power utilization efficiency between a TENG and a lithium battery was achieved with an optimizing circuit.^[21b] Whereas, difficulties in designing this circuit into flexible or wearable components still require further research.

Our approach for integrated power textile could possibly reduce or eliminate the frequent charging of energy-storing devices of wearable electronics. The human motion-charging strategy for self-charging power textile can compensate the energy consumption of the wearable devices and elongate their operational time. Unlike the solar and thermoelectric energy, this self-charging power textile is independent of the weather. Therefore, it can replace or compensate the current strategies of integration between solar, thermoelectric, piezoelectric energy harvesting, and electrochemical energy storage.

In conclusion, we demonstrated a self-charging power textile, which can harvest human motion energy with a TENG cloth and store energy with yarn-type supercapacitors. Our approach for yarn supercapacitors, by converting common fabric yarns into conductive and capacitive electrodes with conformal Ni-coating and subsequent rGO coating, achieved electrochemical performances that rival or improve upon some of the best reported yarn (or fiber) supercapacitors: high specific capacitance (72.1 mF cm^{-2}), stable cycling performances (96% capacitance retention in 10 000 cycles), high areal energy density ($1.60 \mu\text{Wh cm}^{-2}$) and power density (2.42 mW cm^{-2}), and excellent flexibility (no degradation for 180° bending for 1000 times). Meanwhile, we developed a fabric TENG that was demonstrated being capable of harvesting human motion energy. The self-charging power textile was then fabricated by

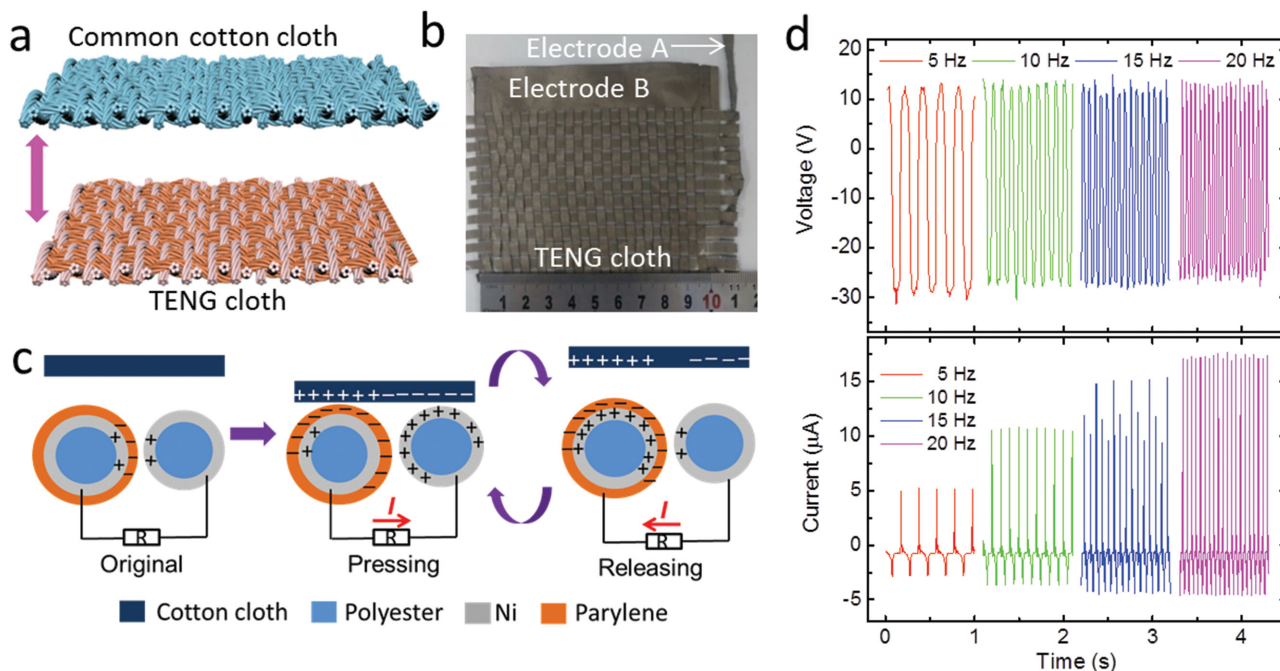


Figure 4. The triboelectric nanogenerator (TENG) cloth. a) Scheme of a TENG cloth moving in contact-separation mode with a common cotton cloth. b) The photograph of a woven TENG cloth. c) Scheme of the working mechanism of the TENG cloth. d) The output open-circuit voltage (upper plot) and short-circuit current (bottom plot) of the TENG cloth in contact-separation motion with a common cotton cloth at different frequencies (5–20 Hz).

weaving the yarn supercapacitors together with a fabric TENG into a single cloth. Proof-of-concept demonstration of the motion-charging process was carried out by charging the yarn supercapacitors by the contact-separation motions between the TENG cloth and a common cotton cloth at different frequencies. Owing to the excellent flexibility and weavability of both the yarn supercapacitors and the fabric TENG, this power textile is possibly incorporated into complicated and fashionable cloths, but efforts are required to design rigid components like rectifier and impedance-optimizing circuit into wearables. Moreover, the facile synthesis of our yarn supercapacitors and fabric TENG with cheap starting materials enables the scale-up facility and cost-effective commercialization. In summary, we have developed novel approaches for yarn supercapacitors and self-charging power textiles that integrate TENG cloths and yarn supercapacitors in an individual fabric. Our scalable strategies for conductive fabrics, capacitive energy-storing yarns, and energy-harvesting wears could greatly promote the progress of wearable electronics.

Experimental Section

Fabrication of the rGO-Ni-Yarn: Polyester yarn with diameter of 0.5 mm was used as the starting substrate for the synthesis of rGO-Ni-yarn. The Ni-coating was prepared by electroless plating similar to our previous report. Polyester yarn was first thoroughly cleaned by abundant acetone and deionized (DI) water with a bath sonicator. Subsequently, it was sensitized by aqueous solution with $10 \text{ g L}^{-1} \text{ SnCl}_2$ and $40 \text{ mL L}^{-1} \text{ 38\% HCl}$, and then activated with an aqueous solution with $0.5 \text{ g L}^{-1} \text{ PdCl}_2$ and $20 \text{ mL L}^{-1} \text{ 38\% HCl}$ at room temperature for 10 min, respectively. After rinsing in DI water, the seeded polyester cloth was immersed in a 0.1 M NiSO_4 aqueous solution for electroless plating

at room temperature for 12 h. After the coating, the Ni-cloth was washed with DI water and then dried in vacuum oven.

Then, the rGO coating was applied on top of the Ni coating. First, Ni-coated polyester yarn was immersed in a $5 \text{ mg mL}^{-1} \text{ GO}$ dispersion (Nanjing XFNANO Materials Tech Co., Ltd) for hydrothermal reaction at $80 \text{ }^\circ\text{C}$ for 6 h. The yarn with spontaneously formed rGO hydrogel film was then further reduced in a 0.1 M ascorbic acid at $90 \text{ }^\circ\text{C}$ for 2 h. Finally, the obtained rGO-Ni-yarn was washed with DI water and dried in vacuum oven.

Fabrication of the Yarn Supercapacitor. Gel-type electrolyte was first prepared. 4 g of PVA (M_w 89 000–98 000) was added into 40 mL of 1 M phosphoric acid, and the mixed solution was kept stirring at $90 \text{ }^\circ\text{C}$ for 1 h.

All-solid-state yarn supercapacitor was assembled with two rGO-Ni-yarns and the gel-type electrolyte. The rGO-Ni-yarn was first immersed in the electrolyte for 30 min, and then dried for 2 h in the air. Subsequently, two rGO-Ni-yarns were assembled in parallel by adding more electrolyte. The yarn supercapacitor was dried in the hum hood overnight before the test.

Fabrication of the TENG Cloth: First, common polyester cloth was coated with conformal Ni coating according to the above processes. Then, parylene was coated on the top of Ni by chemical vapor deposition method with Dichloro-[2,2]-paracyclophane as the source. Subsequently, a $10 \times 10 \text{ cm}$ TENG cloth was woven by using Ni-coated cloth straps and parylene-Ni-coated cloth straps as longitudes and altitudes, respectively. All Ni-coated straps were connected as one electrode, and all parylene-Ni-coated straps were connected as another.

Apparatus for Characterizations: The electrochemical performance was measured by an electrochemical work station (CHI 660E). The output short current and open-circuit voltage of the TENG cloth were measured by a Stanford low-noise current preamplifier (Model SR570) and a Keithley electrometer (Keithley 6514), respectively. XRD measurements were performed with a Panalytical instrument (X'Pert θ Powder). Raman spectra were measured by a confocal Raman spectrometer (HORIBA LabRAM HR Evolution). SEM was taken with a Hitachi SU8200.

Calculation of Electrochemical Performances: All electrochemical performances were tested in a two-electrode configuration with PVA/

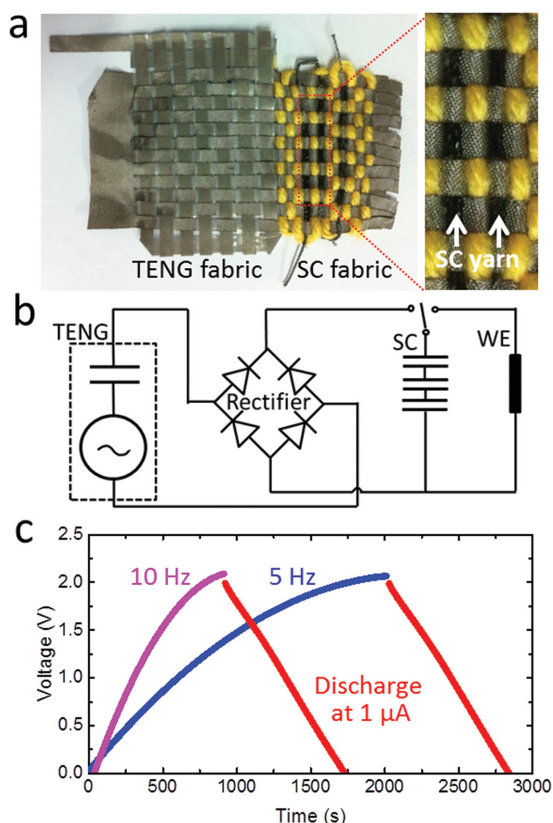


Figure 5. The self-charging power textile. a) The photograph of a self-charging power textile woven with a TENG fabric and a yarn supercapacitor (SC) fabric. The enlarged view of the SC fabric shows two black yarn supercapacitors. b) The equivalent circuit of the self-charging power textile for wearable electronics (WE). c) The voltage profile of three yarn supercapacitors in series charged by the TENG fabrics at motion frequencies of 5 and 10 Hz, and discharged at $1 \mu\text{A}$.

H_3PO_4 as solid electrolyte. Length capacitances obtained for discharging profiles and CV curves were respectively derived by

$$C_{L,\text{electrode}} = \frac{2It}{UL} \quad (1)$$

$$C_{L,\text{electrode}} = \frac{\int_0^U i(u) du}{U\nu L} \quad (2)$$

where I is the discharging current, t is the discharging time, U is the cutoff voltage (i.e., 0.8 V), ν is the scanning rate, and L is the length of tested yarn supercapacitor. Areal capacitances can be calculated by

$$C_{A,\text{electrode}} = C_{L,\text{electrode}} / \pi D \quad (3)$$

where D is the diameter of the rGO-Ni-yarn and is measured to be about $574 \mu\text{m}$ from the SEM image. The areal energy density and power density of the yarn supercapacitor device were obtained by

$$E_{A,\text{device}} = \frac{C_{A,\text{electrode}} U^2}{8 \times 3600} \quad (4)$$

$$P_{A,\text{device}} = \frac{E_{A,\text{device}} \times 3600}{t} \quad (5)$$

where t is the discharging time when calculated from discharging profiles, or the scanning time when calculated from CV curves.

Supporting Information

Supporting Information is available from the Wiley Online Library or from the author.

Acknowledgements

X.P. and L.L. contributed equally to this work. The authors thank for the support from the “thousands talents” program for pioneer researcher and his innovation team, China, National Natural Science Foundation of China (Grant No. 51432005).

Received: September 8, 2015

Revised: October 3, 2015

Published online:

- [1] Z. L. Wang, *Adv. Mater.* **2012**, *24*, 4632.
- [2] a) X. Wang, X. Lu, B. Liu, D. Chen, Y. Tong, G. Shen, *Adv. Mater.* **2014**, *26*, 4763; b) K. Xie, B. Wei, *Adv. Mater.* **2014**, *26*, 3592.
- [3] a) A. S. Arico, P. Bruce, B. Scrosati, J.-M. Tarascon, W. Van Schalkwijk, *Nat. Mater.* **2005**, *4*, 366; b) P. Simon, Y. Gogotsi, B. Dunn, *Sci. Mag.* **2014**, *343*, 1210; c) P. Simon, Y. Gogotsi, *Nat. Mater.* **2008**, *7*, 845; d) P. Yang, X. Xiao, Y. Li, Y. Ding, P. Qiang, X. Tan, W. Mai, Z. Lin, W. Wu, T. Li, H. Jin, P. Liu, J. Zhou, C. P. Wong, Z. L. Wang, *ACS Nano* **2013**, *7*, 2617.
- [4] a) D. Yu, Q. Qian, L. Wei, W. Jiang, K. Goh, J. Wei, J. Zhang, Y. Chen, *Chem. Soc. Rev.* **2015**, *44*, 647; b) W. Zeng, L. Shu, Q. Li, S. Chen, F. Wang, X. M. Tao, *Adv. Mater.* **2014**, *26*, 5310.
- [5] Z. Xu, C. Gao, *Nat. Commun.* **2011**, *2*, 571.
- [6] M. Zhang, K. R. Atkinson, R. H. Baughman, *Science* **2004**, *306*, 1358.
- [7] a) L. Kou, T. Huang, B. Zheng, Y. Han, X. Zhao, K. Gopalsamy, H. Sun, C. Gao, *Nat. Commun.* **2014**, *5*, 3754; b) S. Chen, W. Ma, Y. Cheng, Z. Weng, B. Sun, L. Wang, W. Chen, F. Li, M. Zhu, H.-M. Cheng, *Nano Energy* **2015**, *15*, 642.
- [8] a) J. A. Lee, M. K. Shin, S. H. Kim, H. U. Cho, G. M. Spinks, G. G. Wallace, M. D. Lima, X. Lepró, M. E. Kozlov, R. H. Baughman, *Nat. Commun.* **2013**, *4*, 1970; b) J. Ren, W. Bai, G. Guan, Y. Zhang, H. Peng, *Adv. Mater.* **2013**, *25*, 5965; c) J. Ren, L. Li, C. Chen, X. Chen, Z. Cai, L. Qiu, Y. Wang, X. Zhu, H. Peng, *Adv. Mater.* **2013**, *25*, 1155; d) Z. Yang, J. Deng, X. Chen, J. Ren, H. Peng, *Angew. Chem., Int. Ed.* **2013**, *52*, 13453.
- [9] a) Y. Huang, H. Hu, Y. Huang, M. Zhu, W. Meng, C. Liu, Z. Pei, C. Hao, Z. Wang, C. Zhi, *ACS Nano* **2015**, *9*, 4766; b) T. Chen, L. Qiu, Z. Yang, Z. Cai, J. Ren, H. Li, H. Lin, X. Sun, H. Peng, *Angew. Chem., Int. Ed.* **2012**, *51*, 11977; c) Y. Fu, H. Wu, S. Ye, X. Cai, X. Yu, S. Hou, H. Kafafy, D. Zou, *Energy Environ. Sci.* **2013**, *6*, 805; d) D. Zhang, M. Miao, H. Niu, Z. Wei, *ACS Nano* **2014**, *8*, 4571.
- [10] a) Y. Fu, X. Cai, H. Wu, Z. Lv, S. Hou, M. Peng, X. Yu, D. Zou, *Adv. Mater.* **2012**, *24*, 5713; b) X. Xiao, T. Li, P. Yang, Y. Gao, H. Jin, W. Ni, W. Zhan, X. Zhang, Y. Cao, J. Zhong, *ACS Nano* **2012**, *6*, 9200.
- [11] K. Jost, D. P. Durkin, L. M. Haverhals, E. K. Brown, M. Langenstein, H. C. De Long, P. C. Trulove, Y. Gogotsi, G. Dion, *Adv. Energy Mater.* **2015**, *5*, DOI: 10.1002/aenm.201401286.
- [12] a) F.-R. Fan, Z.-Q. Tian, Z. L. Wang, *Nano Energy* **2012**, *1*, 328; b) Z. L. Wang, *ACS Nano* **2013**, *7*, 9533; c) Z. L. Wang, *Faraday Discuss.* **2014**, *176*, 447.
- [13] a) G. Zhu, B. Peng, J. Chen, Q. Jing, Z. L. Wang, *Nano Energy* **2014**, *14*, 126; b) X. Pu, L. Li, H. Song, C. Du, Z. Zhao, C. Jiang, G. Cao, W. Hu, Z. L. Wang, *Adv. Mater.* **2015**, *27*, 2472.

- [14] N. Liu, W. Ma, J. Tao, X. Zhang, J. Su, L. Li, C. Yang, Y. Gao, D. Golberg, Y. Bando, *Adv. Mater.* **2013**, *25*, 4925.
- [15] a) X. Cao, D. Qi, S. Yin, J. Bu, F. Li, C. F. Goh, S. Zhang, X. Chen, *Adv. Mater.* **2013**, *25*, 2957; b) U. N. Maiti, J. Lim, K. E. Lee, W. J. Lee, S. O. Kim, *Adv. Mater.* **2014**, *26*, 615; c) Z.-J. Fan, W. Kai, J. Yan, T. Wei, L.-J. Zhi, J. Feng, Y.-m. Ren, L.-P. Song, F. Wei, *ACS Nano* **2010**, *5*, 191.
- [16] K. N. Kudin, B. Ozbas, H. C. Schniepp, R. K. Prud'Homme, I. A. Aksay, R. Car, *Nano Lett.* **2008**, *8*, 36.
- [17] K. Wang, Q. Meng, Y. Zhang, Z. Wei, M. Miao, *Adv. Mater.* **2013**, *25*, 1494.
- [18] G. Huang, C. Hou, Y. Shao, B. Zhu, B. Jia, H. Wang, Q. Zhang, Y. Li, *Nano Energy* **2015**, *12*, 26.
- [19] Y. Meng, Y. Zhao, C. Hu, H. Cheng, Y. Hu, Z. Zhang, G. Shi, L. Qu, *Adv. Mater.* **2013**, *25*, 2326.
- [20] Q. Meng, K. Wang, W. Guo, J. Fang, Z. Wei, X. She, *Small* **2014**, *10*, 3187.
- [21] a) S. Niu, Y. Liu, Y. Zhou, S. Wang, L. Lin, Z. L. Wang, *IEEE Trans. Electron Devices* **2015**, *62*, 641; b) X. Pu, M. Liu, L. Li, C. Zhang, Y. Pang, C. Jiang, L. Shao, W. Hu, Z. L. Wang, *Adv. Sci.* **2015**, DOI: 10.1002/advs.201500255.